Full-potential linear-muffin-tin-orbital calculations of the magnetic properties of rare-earth–transition-metal intermetallics. II. $Nd_2Fe_{14}B$

K. Hummler and M. Fähnle
Institut für Physik, Max-Planck-Institut für Metallforschung, Heisenbergstrasse 1, 70569 Stuttgart, Germany
(Received 7 April 1995)

The local magnetic moments and hyperfine fields, the intersublattice exchange fields, the electric field gradients, and the crystal field parameters are calculated for the technologically important hard-magnetic compound $Nd_2Fe_{14}B$ by the full-potential linear-muffin-tin-orbital method in local-spin-density approximation. The results are analyzed and compared with data from other theories and experiments.

I. INTRODUCTION

In Ref. 1 (hereafter denoted as paper I) we described a computational scheme based on the full-potential linear-muffin-tin-orbital method (FLMTO) and the local-spin-density-approximation (LSDA) for the treatment of rare-earth–transition-metal intermetallics. These materials are interesting from a fundamental point of view, because their magnetic properties are determined both by the highly correlated, strongly localized $4f$ states and by the less correlated, less localized valence states. They are also appealing from a technological point of view due to their potential application as permanent magnets.[2]

Various parameters of the two-sublattice model[2] of these materials were calculated in Ref. 1 for the technologically important series RCo_5 (R=rare-earth atom), i.e., local magnetic moments, intersublattice exchange fields, crystal field parameters A_n^m as well as local magnetic hyperfine fields and electric field gradients. The crystal field parameters are very important quantities, because they determine the rare-earth contribution to the magnetocrystalline anisotropy, which is sometimes very large in these materials and which is one of the major features for the technological application as permanent magnets.[2] The experimental determination of the crystal field parameters, however, is rather complicated, because it requires a multiparameter fit to experimental data which is far from being unambiguous (Sec. IV of paper I). To facilitate the multiparameter fits in complicated intermetallics, it is sometimes assumed (Sec. III C) that the crystal field parameters A_2^0 at crystallographically different R sites are proportional to the electric field gradients which are directly measurable for instance by NMR or Mössbauer experiments. Therefore, in the present paper special emphasis is put on the crystal field parameters and the electric field gradients.

In paper I it was demonstrated that for a reliable theoretical determination of the crystal field parameters it is indispensable to refrain from any approximation for the effective crystal potential. This means that the very efficient atomic-sphere approximation[3–17] (ASA) which is able to obtain reliable results for the local magnetic moments, the local magnetic hyperfine fields and in many cases also for the intersublattice exchange interactions (a review is given in Ref. 12) does not suffice. We therefore apply the FLMTO method, which we described in paper I. Furthermore, it was demonstrated in paper I that the application of the LSDA to the case of rare-earth–transition-metal intermetallics introduces large uncertainties for the lowest-order crystal field parameter A_2^0 which cannot be totally removed but at least drastically reduced by physically motivated measures. Finally, it was shown that the crystal field parameter A_2^0 and the electric field gradient at the rare-earth site depend very strongly on the orientation of the aspherical $4f$ charge density in contrast to the basic assumption of the two-sublattice model. As a consequence, the quantities A_2^0 obtained from a multiparameter fit to experimental data (based on the assumption that there is no dependence on orientation) represent effective parameters which may be different for different experiments. Our guess is that we may obtain a representative effective parameter by disregarding the asphericity of the $4f$ charge density (when calculating the effective potential), and we will proceed on the line in papers II and III.

In the present paper II we apply our computational method to the case of $Nd_2Fe_{14}B$, which is the technologically most important representative[2] of the series $R_2Fe_{14}B$. This material has an advantageous economical feature when compared to the compound $SmCo_5$ mainly used as hard magnetic material before 1984 because it is based on Fe which is much cheaper than Co. Several *ab initio* calculations of the magnetic properties of these materials were performed[3–17] within the framework of the ASA calculations, a review is given in Ref. 12. One of the most valuable features of $Nd_2Fe_{14}B$ is the very high magnetocrystalline anisotropy which is related to the crystal field parameters. To obtain reliable results also for the crystal field parameters, we now apply the FLMTO method. Because of the large number (68) of atoms in the unit cell, so far nobody has attempted a full-potential calculation for this compound.

II. DETAILS OF THE CALCULATIONS

The calculations were performed by the full-potential linear-muffin-tin-orbital method (FLMTO) described in paper I within the framework of the local-spin-density approximation. For details of the calculations and for the meaning of the various parameters given below we refer to paper I. Three k points in the irreducible part of the Brillouin zone of the very large elementary unit cell were used. Because of the large number of atoms in the supercell it was impossible to check the convergence with respect to the number of k points

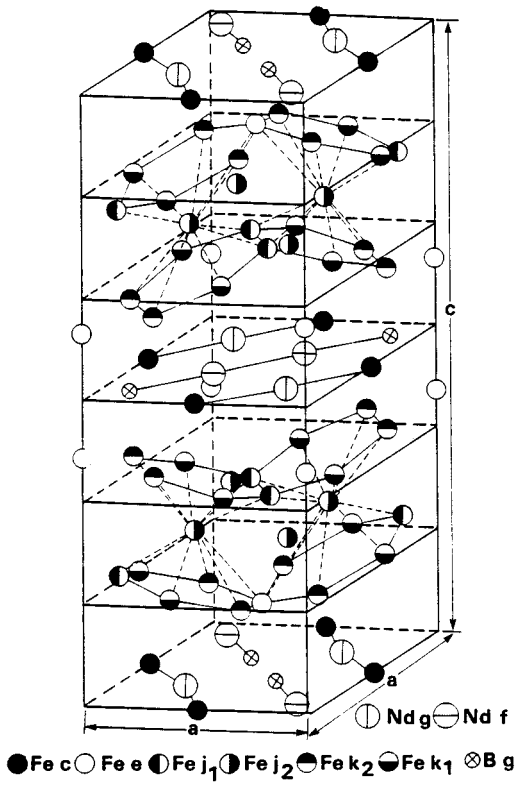

FIG. 1. Tetragonal unit cell of $Nd_2Fe_{14}B$. The c/a ratio is exaggerated to emphasize the puckering of the iron layers. After Herbst *et al.* (Ref. 21), but with the site notation of Shoemaker *et al.* (Ref. 19) used in the present paper.

by going to larger numbers. However, converted to the different number of atoms, the corresponding number of k points in the reducible Brillouin zone corresponds to a number of k points in the reducible Brillouin zone of the RCo_5 elementary cell for which satisfactory convergence was obtained for the series RCo_5 in paper I. The angular momentum cutoffs were $(l_B,l_T,2l_W)=(2,7,8)$ for the Nd sites and (2,6,8) for the other sites. (Confining to $l_T=4$ affected mainly the crystal field parameters A_2^m which are then modified by typically 10%.) A two-κ calculation was performed for the valence band, with $\kappa^2=-0.9$ Ry for the $5p$ states at Nd and $\kappa^2=0.4$ Ry (corresponding to the center of gravity of the occupied part of the valence band) for the other states. It is expected from Table IV of paper I that a two-κ calculation with the $5p$ states included in the valence band yields reliable values for all quantities except for the crystal field parameters A_2^m. We used for the augmentation energies the values κ^2 for $l>l_B$ and the respective centers of gravity of the occupied part of the l-projected band for $l\leqslant l_B$, except for the $4f$ states (-2 Ry) and the $6p$ states ($D_{6p}=1.9$). The $4f$ core states are evaluated in the spherically averaged effective potential for $D_{4f}=-\infty$ at the surface of the muffin-tin spheres around the Nd atom (Sec. III E 1 of paper I), and a spherically symmetric $4f$ core according to Eqs. (11)–(15) of paper I was assumed for the calculation of the effective potential.

The tetragonal elementary unit cell of $Nd_2Fe_{14}B$ contains 68 atoms, 6 crystallographically inequivalent Fe sites, 2 inequivalent Nd sites, and the B site (see Fig. 1). The structure

TABLE I. Magnetic contact hyperfine fields—B_{hf} in T and magnetic moments in μ_B for $Nd_2Fe_{14}B$ as determined by the present FLMTO calculations and the LMTO-ASA method.[8,12,14]

	$-B_{hf}$		μ_{loc}	
	FLMTO	LMTO-ASA	FLMTO	LMTO-ASA
Fe($16k_1$)	27.6	28.5	2.22	2.18
Fe($16k_2$)	29.2	30.7	2.28	2.38
Fe($8j_1$)	29.9	28.2	2.67	2.59
Fe($8j_2$)	29.8	28.8	2.16	2.30
Fe($4c$)	28.7	28.6	2.43	2.46
Fe($4e$)	26.7	26.4	1.96	2.03
B($4f$)	3.9	4.4	−0.13	−0.19

parameters are taken from Ref. 18, and the site notation of Shoemaker *et al.*[19] is used. For comparison with experiments it is important to note that different site notations exist (the interrelations are discussed in Ref. 20). It should also be noted that in our former papers[7,8,10–12,14,15] the site notation of Herbst *et al.*[21] was used, where j_1 and j_2 sites as well as f and g sites are interchanged as compared to Shoemaker *et al.*[19] In our calculations all magnetic moments are aligned parallel to the crystallographic c axis. In reality, there is a noncollinear spin structure in $Nd_2Fe_{14}B$ (see, for instance, the review of Coey[22]) at very low temperatures, so that our calculations refer to the situation above the spin-reorientation temperature, extrapolated to $T=0$.

III. RESULTS AND COMPARISON WITH OTHER THEORIES AND WITH EXPERIMENTS

A. Magnetic hyperfine fields and magnetic moments

Table I represents the results for the local contact hyperfine fields (i.e., hyperfine fields without orbital and dipolar contributions) and the local magnetic moments in comparison with our previous results[8,12,14] obtained by the linear-muffin-tin-orbital method in atomic-sphere approximation (LMTO-ASA).

For an experimental determination of the magnetic hyperfine fields, several *ad hoc* assumptions must be made to decompose the total Mössbauer spectrum into the subspectra originating from crystallographically different sites. For instance, it is often assumed[23] that the local Fe hyperfine field B_{hf} increases with the number of Fe nearest neighbors, yielding for the hyperfine fields a succession $8j_1>16k_2>16k_1>4e\approx 8j_2>4c$. Our LMTO-ASA calculations[8,12,14] (see Table I) arrived at another succession for the hyperfine fields, with the largest value for the $16k_2$ site and the smallest value for the $4e$ site. It has been demonstrated by an analysis of the highly-resolved Mössbauer spectra of Long *et al.*[23] that an assignment of the largest B_{hf} to the $16k_2$ site would lead to an inconsistency of the relative intensity of the corresponding magnetic sextet with the relative crystallographic degeneracy of this site, so that this site assignment can be excluded—in contrast to our previous LMTO-ASA calculations. In Ref. 14 we assumed that the problem might arise from the neglect of the dipolar and orbital contributions or from a deficiency of the local-spin-density approximation. In the present FLMTO calculations the hyperfine field at the

TABLE II. Components of the EFG at the Nd sites in $Nd_2Fe_{14}B$ (without $4f$ contribution) in the Cartesian coordinate system defined by the axes of the tetragonal unit cell (V_{zz}, V_{xy}) and in the respective principle coordinate system (V_{33}, V_{22}). All numbers are given in units of 10^{21} V m^{-2}. The table gives also the NMR results (Ref. 26) for $Nd_2Fe_{14}B$ (note that in Ref. 26 the symbols V_{zz} and V_{cc} correspond to our symbols V_{33} and V_{zz}, respectively, and that the site notation of Herbst *et al.* (Ref. 21) is used). Comparison is also made with results for $Gd_2Fe_{14}B$ from ASW-ASA calculations and Mössbauer experiments.

	$4f$				$4g$			
	V_{zz}	V_{xy}	V_{33}	V_{22}	V_{zz}	V_{xy}	V_{33}	V_{22}
FLMTO $5p$ valence	−8.57	−1.07	−8.57	5.35	−7.05	6.00	9.52	−7.05
FLMTO $5p$ semicore	−10.74	2.48	−10.74	7.85	−9.99	9.17	14.17	−9.99
LMTO-ASA (Ref. 25)	−8.8 to −6.4				−9.1 to −8.4			
NMR (Ref. 26)	−6.7		−6.7		−2.5		8.29	
ASW-ASA (Ref. 3)	−8.8				−7.7			
Mössbauer (Ref. 27)	−7.59	−2.50	−7.59	6.30	−7.70	7.56	11.41	−7.70

$16k_2$ site is slightly decreased as compared to the LMTO-ASA calculation and the hyperfine fields at the $8j_1$ and $8j_2$ sites are slightly increased (Table I). As a result, the largest hyperfine fields now are at the j_1 and j_2 sites rather than at the $16k_2$ site. However, the hyperfine fields at the two j sites are so close in value that the experimental Mössbauer line[23] at 6 mm/sec should appear with a relative intensity of 16 and not of 8 as observed experimentally. As outlined in Ref. 14, one obviously must consider the dipolar and orbital contributions and must cure the deficiency of the local spin-density approximation in order to arrive at decisive calculations. In agreement with the LMTO-ASA calculations and with the sign assignment of various experimentalists (see Ref. 14), the $4e$ site rather than the $4c$ site (as suggested by Ref. 23) exhibits by far the smallest hyperfine field. This possibly indicates[14] that the number of neighboring B atoms is more important for the value of $B_{\rm hf}$ than the number of neighboring Fe atoms.

Our present data for the local magnetic moments agree well with the results from our previous LMTO-ASA calculations[8,12,14] which are extensively compared with the experimental data in Refs. 8, 12, 14. The total magnetic moment per elementary unit cell of $37.5\mu_B$ is close to the LMTO-ASA value[8,14] of $37.8\mu_B$ and the experimental value[24] of $37.6\mu_B$. The magnetic moment per unit cell in the interstitial space between the muffin-tin spheres is $-0.69\mu_B$ only, indicating that the spin density is well localized at the atoms.

It becomes obvious from Table I that the local magnetic hyperfine fields are not proportional to the local magnetic moments, in contrast to the assumption which is made very often for an analysis of Mössbauer experiments (for a discussion, see Refs. 8, 10–12, and 14).

B. Electric field gradients

Our FLMTO results for the components of the electric-field-gradient (EFG) tensor are shown in Table II, together with results from LMTO-ASA calculations[25] and from augmented-spherical-wave ASW-ASA calculations[3] for $Gd_2Fe_{14}B$. In the ASA calculations only the contribution of the electrons in the atomic sphere surrounding the rare-earth sites is taken into account, and the results depend to some extent on the choice of the respective radii of the atomic spheres, which for multicomponent alloys is not unique. The range of values spanned by the LMTO-ASA data of Table II gives a feeling for this dependence. Furthermore, the $5p$ states are treated as core states in the ASA calculations, whereas in the FLMTO calculation they are considered either as semicore states or as valence states. It has been shown in paper I that it is indispensable to include the $5p$ states of the rare-earth atoms into the valence band in order to obtain accurate values for the EFG and the crystal field parameters. For $Nd_2Fe_{14}B$, the difference between these two calculations is smaller than for the series RCo_5 (paper II) but still considerable. In Table II we compare also with experimental results. Kapusta *et al.*[26] determined the EFG of $Nd_2Fe_{14}B$ at 4.2 K from spin-echo NMR spectra. Two problems should be considered for a comparison of our theory with these experiments. First, one should take into account that at 4.2 K there is a noncollinear spin structure in $Nd_2Fe_{14}B$, whereas we assume a spin alignment along the c axis for our calculations. As shown in Sec. III D of paper I, the EFG may depend rather sensitively on the orientation of the magnetization if dealing with an aspherical $4f$ charge density. This should result in a temperature dependence of the EFG below the spin-reorientation temperature, which should be easily detectable in experiments. Second, the electric field gradient at the Nd site is dominated by the contribution from the aspherical $4f$ charge density, and the separation of this contribution in the analysis of the experimental data requires assumptions which may introduce uncertainties for the value of the remaining EFG. Because of these two problems, we also compare with the experimental values from Mössbauer experiments[27] at 4.2 K for $Gd_2Fe_{14}B$, where there are no

TABLE III. Results from the present FLMTO calculations for the crystal field parameters A_n^m (total as well as valence and lattice contributions) and for $A_n^m\langle r^n\rangle_{4f}$ at the Nd sites in $Nd_2Fe_{14}B$. Upper part: Nd($4f$) site; lower part: Nd ($4g$) site.

n,m	2,0	2,−2	4,0	4,−2	4,4	6,0	6,−2	6,4	6,−6
A_n^m[Ka$_0^{-n}$]	476	−640	−20	30	46	−0.2	0.0	−1.5	0.5
Valence	497	426	−19	19	33	0.0	0.1	0.2	−0.1
Lattice	−22	−1066	−0.8	11	13	−0.2	−0.1	−1.6	0.5
$A_n^m\langle r^n\rangle_{4f}$[K]	540	−727	−54	82	125	−2.2	0.3	−15	5
n,m	2,0	2,−2	4,0	4,−2	4,4	6,0	6,−2	6,4	6,−6
A_n^m[Ka$_0^{-n}$]	284	709	−18	−31	−43	−0.3	0.4	−2.3	0.0
Valence	643	1454	−20	−10	−54	0.0	0.1	0.1	0.1
Lattice	−359	−745	2.2	−21	11	−0.3	0.3	−2.3	−0.1
$A_n^m\langle r^n\rangle_{4f}$[K]	323	807	−50	−85	−117	−2.7	3.9	−24	0.1

contributions from the $4f$ shell to the EFG. It is sometimes assumed that the EFG varies only slightly across the series of a rare-earth compound. However, the fact that the asphericity of the $4f$ charge density has a big effect on the EFG (Section III D of paper I) and that the degree of this asphericity varies strongly across the series throws some doubts on this assumption. This must be taken into account when comparing $Nd_2Fe_{14}B$ with $Gd_2Fe_{14}B$.

In Table II we discuss the components $V_{zz}=V_{cc}$ and $V_{xy}=V_{ab}$ of the EFG in the Cartesian coordinate system spanned by the axes a,b,c of the tetragonal unit cell, as well as the components V_{22} and V_{33} in the local principal coordinate systems at the $4f$ and the $4g$ sites, respectively (with $V_{11}+V_{22}+V_{33}=0$). The signs and the succession in absolute values of the EFG agree between theories and experiments. Whereas all the theoretical results and the Mössbauer results for $Gd_2Fe_{14}B$ yield a similar value of V_{zz} for the two rare-earth sites, there is a drastic difference between the Nd sites according to the NMR experiments. Calculations and experiments find larger absolute values of V_{33} for the $4g$ site than for the $4f$ site.

C. The crystal field parameters

Table III exhibits our theoretical results for the crystal field parameters A_n^m in comparison with experimental data. It should be noted again that the values of the A_2^m as obtained from the present two-κ calculation are expected to be less accurate than the data for the other quantities. However, we think that the order of magnitude, the signs and the differences between the two Nd sites are correctly reproduced also for the A_2^m. The sign of A_n^m for $m\neq 0$ depends on the question which one of the four respective equivalent Nd sites is considered and how the translation vectors $\mathbf{T}_i$ of the tetragonal unit cell are oriented with respect to the Cartesian axes for which the $4f$ multipole moments occurring in the expression for the magnetic anisotropy [Eq. (3) of paper I] are defined. In our calculations the $\mathbf{T}_i$ are aligned parallel to these Cartesian axes and the A_n^m are evaluated at the Nd ($4f$) site $0.64278\mathbf{T}_1+0.35722\mathbf{T}_2+0.5\mathbf{T}_3$ and at the Nd($4g$) site $0.76984\mathbf{T}_1+0.76984\mathbf{T}_2+0.5\mathbf{T}_3$, using the structural parameters of Ref. 18.

In contrast to the system RCo_5 (paper I), where A_2^0 was determined both by the valence and the lattice contribution and where A_n^m for $n>2$ was dominated by the lattice contribution, no such systematics appears for $Nd_2Fe_{14}B$. For the Nd($4f$) site the valence contribution is dominant, whereas for the Nd($4g$) site both the valence and the lattice contribution are relevant for A_2^0. In contrast, the EFG is totally determined by the valence contribution, which in turn is not proportional to the valence contribution to A_2^0 (see Sec. I D of paper I). Altogether, A_2^0 is by no means proportional to the EFG, in contrast to the assumption which is often made for an analysis of experimental data (see below). The importance of both the valence contribution (which is totally neglected in the so-called point-charge models; see Sec. I D of paper I) and the lattice contribution for the case of $Nd_2Fe_{14}B$ was first emphasized by the calculations of Zhong and Ching[28] (which, however, were based on a non-self-consistent effective potential, which of course strongly affects the accuracy of the quantitative results). In the following years, calculations based on the ASA were performed,[3–18] which considered only the valence contributions. Although they used a self-consistent effective potential, the accuracy was limited by the application of this potential approximation. Nevertheless, the results for A_2^0 across the series $R_2Fe_{14}B$ were in semiquantitative agreement[7,10–12] with the experimental data, possibly because for the $R(4f)$ site A_2^0 is indeed dominated by the valence contribution. In spite of this, we are convinced that for an accurate determination of the A_n^m a highly accurate full-potential calculation of the valence and the lattice contribution is required. For instance, the valence contribution to A_2^0 is larger for the $4g$ site than the $4f$ site, in agreement with our former ASA calculations[7,10–12] (note the different site notation in these papers). However, the total value of A_2^0 including the lattice contribution (which is neglected in the ASA calculations) is larger for the $4f$ site than for the $4g$ site.

The experimental determination of the A_n^m proceeds on the same line as described in paper I (Sec. IV C) and exhibits the same problems, i.e., (i) the number of fitting parameters is very large, and the fits to experimental data therefore are far from being unambiguous, and (ii) the fitting parameters represent effective parameters which are different for different experiments. To reduce the number of fitting parameters, *ad hoc* assumptions are often made which are not always justified. For instance, Yamada *et al.*[29] assign the same val-

ues of A_n^m to the Nd($4f$) and the Nd($4g$) site, and Radwański and Franse[30] allow a difference only for A_2^{-2}. In contrast, allowing for differences at the two sites for all A_n^m Zhao and Lee[31] arrive at rather large differences for other representatives of the series $R_2Fe_{14}B$ (they did not investigate $Nd_2Fe_{14}B$), especially for the A_2^{-2}. In our calculations, there are also large differences between the two sites: the A_2^0 values differ by a factor of about 1.7, and the values for A_2^{-2}, A_4^{-4}, and A_4^4 are even of opposite sign (as found by Zhao and Lee for other representatives of the series). Cadogan *et al.*[32] assume that the ratio $A_2^m(f)/A_2^m(g)$ is given by the ratio of the EFG, in contrast to the general statement of the last paragraph. Unfortunately, it is not always possible to find out from the experimental papers which kind of site notation (see Sec. II) was used and how the translation vectors $\mathbf{T}_i$ of the tetragonal unit cell are oriented with respect to the Cartesian axes for the $4f$ multipole moments. We therefore refrain from a more detailed comparison with experimental data.

D. Intersublattice exchange fields

Based on the method outlined in Refs. 9–13 we have determined the intersublattice exchange fields $B_{ex}(4f)$ and $B_{ex}(4g)$ which the transition metal spins exert on the Nd spins at the $4f$ and the $4g$ sites, as well as the exchange field B_{ex}^{Nd} describing the exchange interaction among the Nd spins. The results are $B_{ex}(4f)=364$ T, $B_{ex}(4g)=331$ T, corresponding to a mean value of $B_{ex}=348$ T, and a very small value of $B_{ex}^{Nd}=4$ T. By our LMTO-ASA calculations we obtained[9–13] $B_{ex}=421$ T. For $GdCo_5$ and $SmCo_5$ the exchange fields obtained from the FLMTO and the LMTO-ASA calculations agreed almost perfectly (see Sec. IV B of paper I). The reason for the discrepancy in the case of $Nd_2Fe_{14}B$ is not known. As outlined in Sec. IV C of paper I, the problems for the experimental determination of the A_n^m (Sec. III C) have also an influence on the exchange fields, which are determined simultaneously with the A_n^m in the multiparameter fits. Accordingly, there is a scatter in the experimental values for B_{ex} which ranges from 447 to 554 T (see Refs. 12 and 13). However, all experimental data are larger than the values obtained by the FLMTO and the LMTO-ASA calculation. Analogously, for the series RCo_5 the experimental values of the exchange fields were consistently larger than the theoretical ones for the light representatives of the series (Fig. 5 of paper I). On the other hand, for $GdCo_5$ (paper I) and $Gd_2Fe_{14}B$ LMTO-ASA calculations[9,12,13] and results from inelastic neutron scattering experiments[33,34]) there was perfect agreement between theory and experiment. Our guess therefore is that good fits to the experimental data for the light rare-earth atoms can be also obtained for lower values of the exchange fields and larger values of the A_n^m. Our result $B_{ex}(4f)>B_{ex}(4g)$ agrees with the result from the LMTO-ASA calculations (Ref. 12; in this reference the f and g sites are exchanged by mistake), but is in contrast to the site assignment of Ref. 33.

IV. SUMMARY AND CONCLUSIONS

In this paper we presented results of full-potential electronic structure calculations for the technologically very important intermetallic compound $Nd_2Fe_{14}B$. Because the experimental determination of the various magnetic parameters requires a multiparameter fit to the experimental data which is not unambiguous, it is highly desirable to obtain reliable theoretical results which may be used as fixed input parameters for the analysis of experimental data. The results of our full-potential calculations were compared with those obtained by calculations based on a potential approximation, the so-called atomic-sphere approximation. The following results were obtained.

(i) For the local magnetic moments and hyperfine fields the results of these two types of calculations agree rather well. As in other systems, it turns out that the local magnetic hyperfine fields are not proportional to the local magnetic moments, in contrast to an assumption which is made very often for an analysis of Mössbauer experiments.

(ii) The agreement between the two types of calculations is also good for the electric field gradients, which turn out to be very similar at the two crystallographically different Nd sites. The agreement is less good for the intersublattice exchange field.

(iii) For an accurate determination of the crystal field parameters the use of a full-potential method is indispensable. The crystal field parameters are drastically different for the two crystallographically inequivalent Nd sites, and this must be taken into account for an analysis of experimental data. The results (ii) and (iii) mean that the crystal field parameters are not proportional to the electric field gradients, in contrast to an often used assumption for the data analysis.

ACKNOWLEDGMENT

We are indebted to Dr. S. Savrasov for supplying us with his FLMTO program as a starting point for the development of our FLMTO code. Most of the calculations were performed at the HLRZ in Jülich.

[1] K. Hummler and M. Fähnle, preceding paper, Phys. Rev. B **53**, 3272 (1996).
[2] J. F. Herbst, Rev. Mod. Phys. **63**, 819 (1991).
[3] R. Coehoorn, in *Supermagnets, Hard Magnetic Materials*, Vol. 331 of *NATO Advanced Study Institute, Series C*, edited by G. J. Long and F. Grandjean (Kluwer, Dordrecht, 1991), p. 133.
[4] S. S. Jaswal, Phys. Rev. B **41**, 9697 (1990).
[5] L. Nordström, B. Johansson, and M. S. S. Brooks, J. Appl. Phys. **69**, 5708 (1991).
[6] R. Coehoorn, J. Magn. Magn. Mater. **99**, 55 (1991).
[7] K. Hummler and M. Fähnle, Phys. Rev. B **45**, 3161 (1992).
[8] K. Hummler, T. Beuerle, and M. Fähnle, J. Magn. Magn. Mater. **115**, 207 (1992).
[9] M. Liebs, K. Hummler, and M. Fähnle, Phys. Rev. B **46**, 11 201 (1992).
[10] K. Hummler, M. Liebs, T. Beuerle, and M. Fähnle, Int. J. Mod. Phys. B **7**, 710 (1993).
[11] M. Fähnle, K. Hummler, T. Beuerle, and M. Liebs, in *Computer*

Aided Innovation of New Materials II, edited by M. Doyama, J. Kihara, M. Tanaka, and R. Yamamoto (Elsevier, New York, 1993), p. 209.
[12] M. Fähnle, K. Hummler, M. Liebs, and T. Beuerle, Appl. Phys. A **57**, 67 (1993).
[13] M. Liebs, K. Hummler, and M. Fähnle, J. Magn. Magn. Mater. **124**, L239 (1993).
[14] M. Fähnle, K. Hummler, and T. Beuerle, J. Magn. Magn. Mater. **127**, L278 (1993).
[15] K. Hummler and M. Fähnle, J. Magn. Magn. Mater. **128**, L255 (1993).
[16] R. Coehoorn and K. H. J. Buschow, J. Magn. Magn. Mater. **118**, 175 (1993).
[17] L. Nordström, B. Johansson, and M. S. S. Brooks, J. Phys. Condens. Matter **5**, 7859 (1993).
[18] Struc. Rep. **51A**, 23 (1984).
[19] C. B. Shoemaker, D. P. Shoemaker, and R. Fruchart, Acta Crystallogr. C **40**, 1665 (1984).
[20] R. Fruchart, P. L'Heritier, P. Dalmas de Réotier, D. Fruchart, P. Wolfers, J. M. D. Coey, L. P. Ferreira, R. Guillen, P. Vulliet, and A. Yaouanc, J. Phys. F **17**, 483 (1987).
[21] J. F. Herbst, J. J. Croat, and W. B. Yelon, J. Appl. Phys. **57**, 4086 (1985).
[22] J. M. D. Coey, J. Less-Common Met. **126**, 21 (1986).
[23] G. J. Long, F. Grandjean, and O. A. Pringle, J. Magn. Magn. Mater. **125**, L29 (1993).
[24] D. Givord, H. S. Li, and F. Tasset, J. Appl. Phys. **57**, 4100 (1985).
[25] K. Hummler, diploma work, University of Stuttgart, 1992.
[26] Cz. Kapusta, H. Figiel, G. Stoch, J. S. Lord, and P. C. Riedi, IEEE Trans. Magn. **29**, 2893 (1993).
[27] M. Bogé, G. Czjzek, D. Givord, C. Jeandey, H. S. Li, and J. L. Oddou, J. Phys. F **16**, L67 (1986).
[28] X.-F. Zhong and W. Y. Ching, Phys. Rev. B **39**, 12 018 (1989).
[29] M. Yamada, H. Kato, H. Yamamoto, and Y. Nakagawa, Phys. Rev. B **38**, 620 (1988).
[30] R. J. Radwański and J. J. M. Franse, J. Magn. Magn. Mater. **80**, 14 (1989).
[31] T. S. Zhao and J. I. Lee, J. Appl. Phys. **75**, 3008 (1994).
[32] J. M. Cadogan, J. P. Gavigan, D. Givord, and H. S. Li, J. Phys. F **18**, 779 (1988).
[33] M. Loewenhaupt, I. Sosnowska, A. Taylor, and R. Osborn, J. Appl. Phys. **69**, 5593 (1991).
[34] M. Loewenhaupt and P. Fabi, J. Alloys Compounds **207/208**, 146 (1994).